



### **3.3. Condensation of Vapor Outside Low- and Medium-Finned Trufin Tubes**

This section is concerned with the application of low- and medium-finned Trufin tubes to cases where condensation (including desuperheating and subcooling) is taking place on the finned surface of the tubes. Typical applications for outside condensing include:

*Condensing refrigerants in air conditioning, refrigeration and cryogenic processing systems with cooling water.* Typical refrigerants have heat transfer coefficients from about 150 to 500 Btu/hrft<sup>2</sup>°F; the water coefficient will usually be from 1000 to 1500, so the advantages of using Trufin on the condensing side are clear. Condensing overhead streams for distillation columns in water-cooled condensers. An overhead stream from a distillation column may be composed of essentially one component or it may contain many components. In either case, the condensing coefficient is likely to be less than half of the water coefficient. If the condensing temperature range is very long (for a multi-component mixture, or for a vapor containing a non-condensable gas), a large portion of the total heat transfer may be sensible cooling of the remaining gas or vapor. This coefficient is almost always very low compared to the coolant coefficient, or even the condensing coefficient, making the use of Trufin even more attractive.

*Condensing vapor using a non-aqueous coolant.* In this case, the coefficients of the two fluids may be nearly equal and there might seem to be little advantage in using standard Trufin. However, a doubly enhanced tube such as Turbo-Chil has internal spiral ridges as well as conventional external fins. These ridges enhance the tube side coefficient and the combined enhancement can lead to a very substantial reduction in heat exchanger size.

One application for which Trufin is not recommended is the condensation of water vapor (steam). Because of its high surface tension, water tends to bridge the gaps between the fins and a thick layer is retained on the tube, severely reducing the effective heat transfer coefficient. For this application, Korodense can be advantageous.

#### **3.3.1. Shell and Tube Heat Exchangers for Condensing Applications**

Shell and tube exchangers offer a mechanically feasible way of providing a large heat transfer area in a relatively compact volume. The configuration is strong enough to withstand a wide range of operating conditions commonly encountered in the process and power industries, and offers an enormous number and range of design options to meet most requirements.

The basic construction of the shell and tube exchanger is described in Chapter 1, and we will not repeat that material here. However, there are several special configurations of shell and tube exchanger that are particularly interesting in condensing applications, and these are described in the following paragraphs (15).

Fig. 3.11 shows a typical shell and tube condenser as employed in the process industries. Condensation occurs on the shell-side, the vapor entering through a nozzle at one end and the condensate being removed from the nozzle on the bottom side of the shell at the other. There is also a vent for non-condensable gases at the condensate exit end of the condenser. This configuration is known, by TEMA notation, as an E shell. The drawing shows a fixed tube sheet, two coolant pass arrangement. The baffling is shown in Section AA in the most usual configuration, that is, segmentally cut baffles with a vertical cut and the baffles notched on the bottom to allow drainage of the condensate from one compartment to the next and finally to the condensate exit. However, there has been a recent trend to



# WOLVERINE TUBE HEAT TRANSFER DATA BOOK

use horizontally-cut baffles so that the two-phase flow must go up and over; this arrangement is believed to minimize the possibility of stratification and liquid segregation on the shell-side, but at the cost of additional pressure drop. An impingement plate is shown at the vapor inlet to protect the tubes immediately adjacent to the vapor nozzle from erosion from liquid droplets carried along in the vapor. It is almost universal practice to use an impingement plate at the vapor inlet on a shell-side condenser.

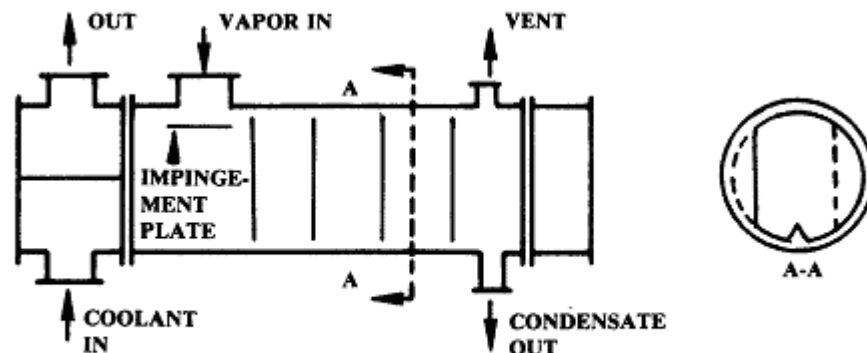


Fig. 3.11 Shell and Tube Exchangers Arranged for Shell-Side Condensation. One Shell-Side Pass, Two Tube-Side Passes.

It is often necessary in heat recovery service (e.g., feed effluent exchangers) to carry out condensation in several exchangers in series. Shell-side condensation in stacked horizontal E shells is the usually preferred design in this case (Fig. 3.12). This arrangement minimizes (but does not eliminate) the possibility of phase segregation and the resultant distortion of the multicomponent vapor-liquid equilibrium profile. It is still important to select a baffle spacing and cut to keep vapor velocities fairly high, and the baffle geometry will often be different for each shell.

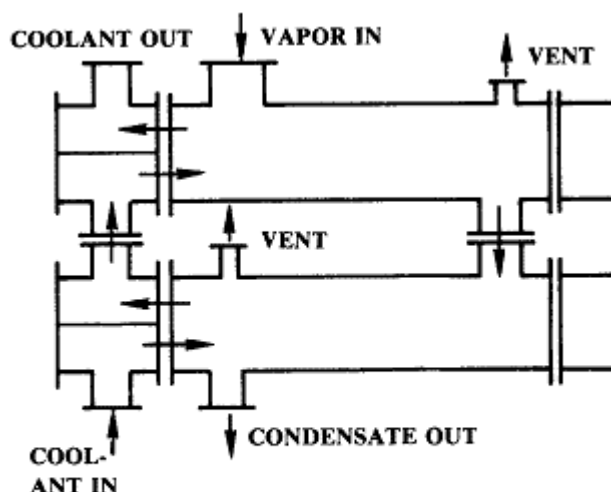


Fig. 3.12 Two 1-2 E Shell Condensers in Series for a Wide Condensing Range Mixture.

Fig. 3.13 shows a somewhat different configuration for shell-side condensation, referred to in the TEMA notation as a G shell. The flow is split into two streams which proceed more or less symmetrically from the center vapor inlet to the ends of the tubes, being guided in this direction by the longitudinal baffle. The flow is then turned around in the end baffle sections and brought back through the lower portion of the tube field; the condensate exits from the central hot well of the condenser. Again, the standard practice is to make the baffle cuts vertical so that the flow is from side to side.

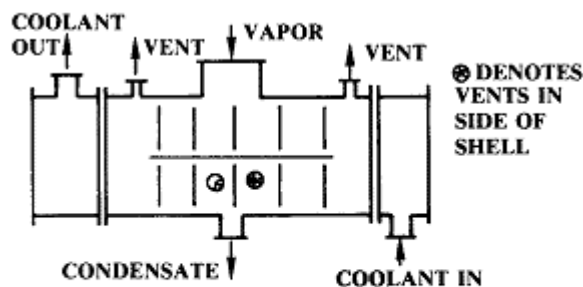


Fig. 3.13 TEMA G Shell used as a Condenser (1-1). One Longitudinal Baffle, and Vertical Cut Transverse Baffles.

Fig. 3.14 shows the TEMA J shell configured as a condenser. The baffle cuts are usually vertical. Dividing the flow and halving the flow distance (compared to the corresponding E shell) results



# WOLVERINE TUBE HEAT TRANSFER DATA BOOK

in a reduction of 60 to 80 percent in pressure drop, a consideration of especial importance in vacuum service. However, the temperature profiles require careful analysis because they are not identical for the two sections.

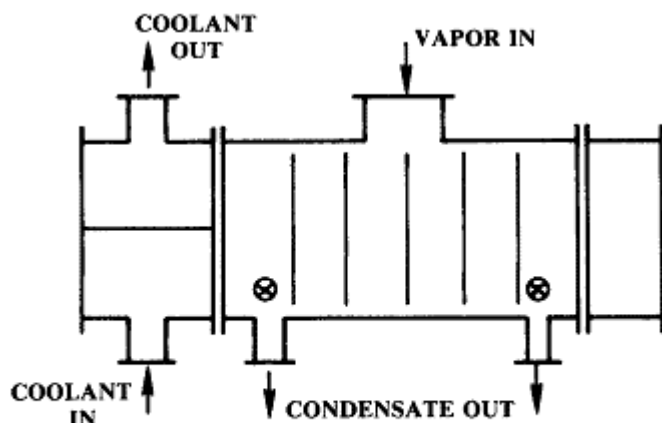


Fig. 3.14 TEMA J Shell Used as a Condenser (1-2). Vertical Cut Baffles Used as Tube Supports.

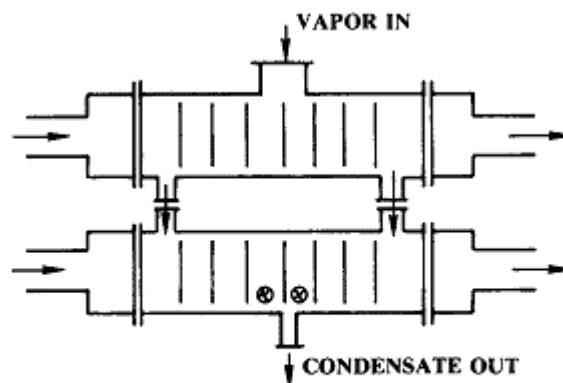


Fig. 3.15 Two J Shells Used in Series for Condensing, with Coolant Flow in Parallel.

J shells can be stacked in series as shown in Fig. 3.15. As drawn, the coolant flow is in parallel to the two shells; this maximizes the effective temperature difference for condensing but can only be used when abundant coolant is available.

Fig. 3.16 shows a further modification of shell-side condensing arrangements, commonly referred to as an H shell. This is effectively a double G shell arrangement, commonly, called a double split flow, and is used to reduce the pressure drop. These units are frequently used for vacuum condensing applications. The transverse baffles have vertical cuts and overlap only enough to insure tube support, i.e., the overlap will ordinarily be two rows of tubes at the vertical centerline of the shell. The configuration shown uses a U tube bundle in order to show possible variant design configurations; however, fixed tube sheet/single tube-side pass and other design options are feasible with this particular shell-side geometry.

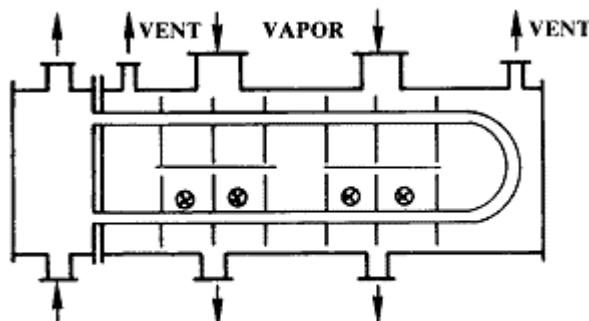


Fig. 3.16 TEMA H Shell in a Condensing Application.

If pressure drop is extremely limited, the usual design choice will be the X shell shown in Fig. 3.17. This arrangement provides that the vapor flow is essentially in cross-flow with the tube bank and is always arranged so that gravity will remove the condensate from the tube surfaces. There must be sufficient clearance between the top of the baffles and the shell to allow the vapor to disperse longitudinally across the entire length of the tubes. Sometimes this is accomplished by putting a large longitudinal vapor nozzle on top of the shell; this arrangement is descriptively referred to as a bathtub nozzle. If adequate space is provided between the tube field and the shell for longitudinal flow of the vapor, each transverse baffle can be a full baffle giving full tube support to the entire bundle. The baffles exist only for tube support, and their spacing is controlled by vibration requirements. The arrangement shown here has a four coolant pass arrangement. The vent for this design would ordinarily be located in the condensate hot well, which would be designed to maintain a vapor/liquid interface below the tube field. The non-condensables would tend to accumulate at the top of the hot well and could be vented from there. Vents at the far end of the



# WOLVERINE TUBE HEAT TRANSFER DATA BOOK

shell would also usually be required in order to permit removal of any non-condensable gases that might otherwise accumulate there and not be swept down to the hot well.

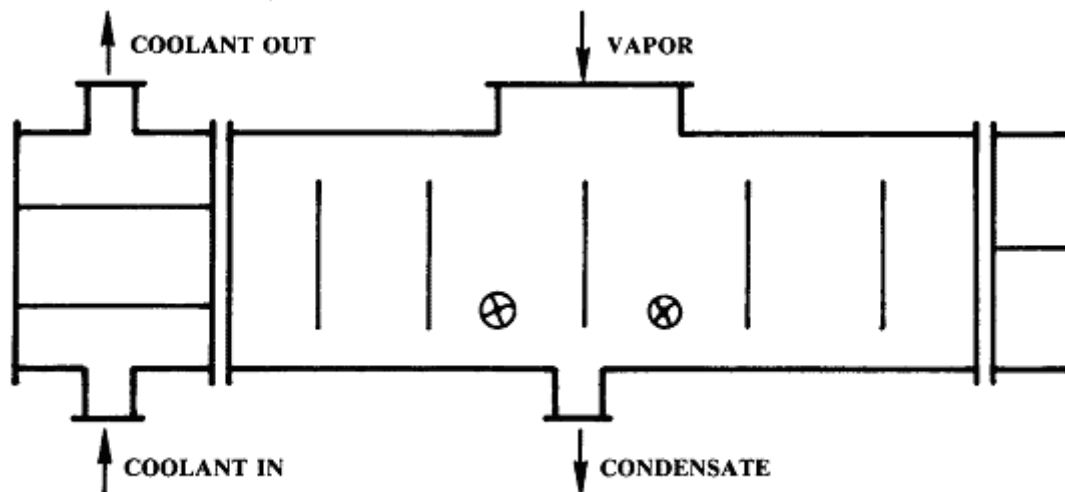


*Fig. 3.17 TEMA X Shell Used for Condensing.*

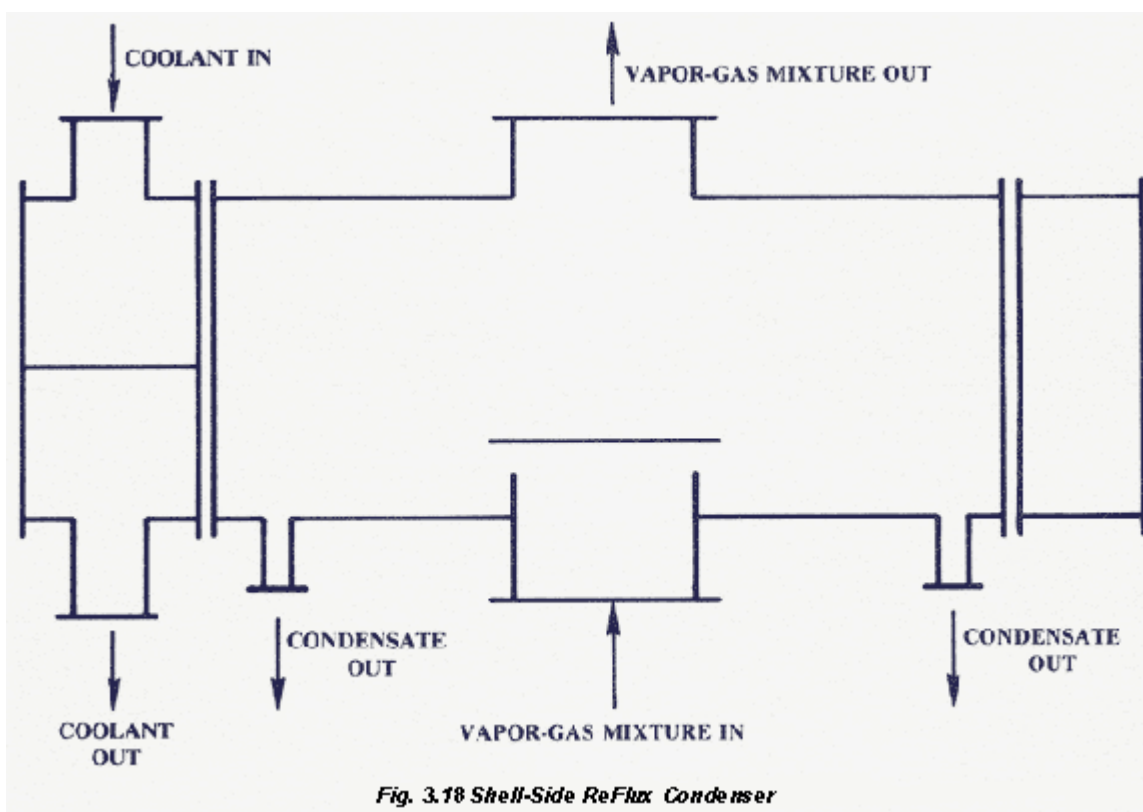


*Fig. 3.18 Shell-Side ReFlux Condenser*

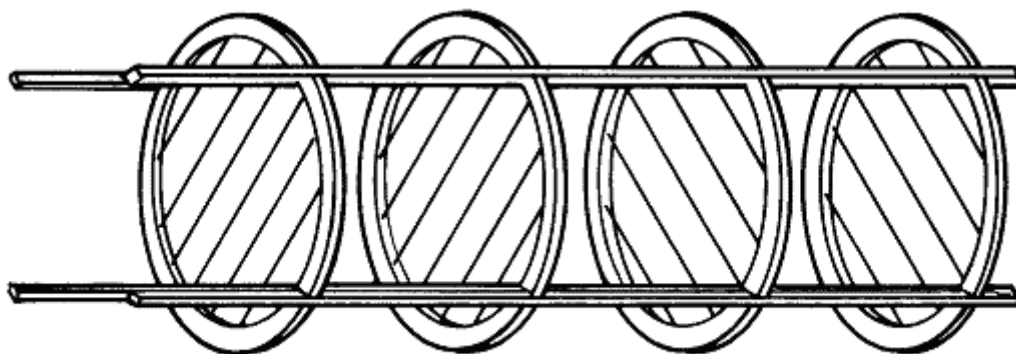
Another design to meet a special need is the shell-side reflux or knock-back condenser shown in Fig. 3.18. A typical application is to partially condense a wide condensing range vapor-gas mixture. The first liquid to condense is carry but will dissolve in the lighter liquid condensed near the top of the bundle. By



# WOLVERINE TUBE HEAT TRANSFER DATA BOOK

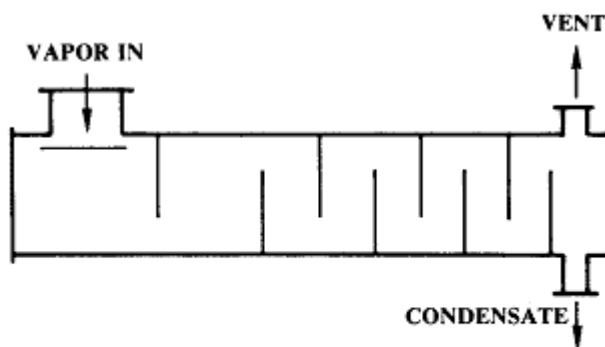
keeping the gas/vapor velocity low (an essential in all reflux condensers), the lighter liquid drains downwards constantly washing off the tarry material.

Fig. 3.19 shows a recent proprietary innovation in shell side condensation in the rod baffle design, licensed by Phillips Petroleum Company (16). In this case, each segmental baffle is replaced by a set of four individual baffles, each one composed of a ring that fits close to but inside the shell, with straight rods extending from one side of the ring baffle to the other. The straight rods are so arranged that they pass between the tube rows with minimum clearance. Every point at which a rod passes next to a tube provides a point of support for that tube in that direction. The rods are arranged so that there are two rows of tubes between each pair of rods in the baffle; the next baffle in line has offset rods passing between the two tube rows that were not individually supported by the previous baffle on that side. The individual baffles are spaced 6 to 8 in. apart, i.e., each tube being supported on all four sides every 24 to 32 in. along the length of the tube. This configuration was first introduced to prevent vibration in an extremely high velocity service but it is now recognized to be at least as valuable for condenser application because of the low pressure drop caused by this particular selection of rod geometry.



*Fig. 3.19 Rod Baffle Arrangement, Used with All TEMA Shell Types.*

Some other shell-side condensing options have considerable application. Fig. 3.20 shows variable baffle spacing on the condensing side. The intention here is to maintain high vapor velocity and therefore shear enhancement of the condensing heat transfer coefficient. Clearly, a fair amount of knowledge on the effect of vapor shear and the ability to predict two-phase flow characteristics on the shell-side is required if this option is to be effectively exercised. This arrangement can be used only when there is a reasonable amount of pressure drop allowed on the condensing side to permit maintaining vapor velocities at a high enough value to get shear enhancement. Removal of non-condensable gases in this geometry is quite positive as long as a vent is located on the exit end of the shell, because this is where the natural flow of the vapors will carry the gas. A computer based rating method is essential to the effective use of this option, and detailed discussion of such applications is beyond the scope of this Manual.



*Fig. 3.20 Variable Baffle Spacing in a Condenser, To Maintain Vapor Shear-Controlled Flow.*





# WOLVERINE TUBE HEAT TRANSFER DATA BOOK

Fig. 3.21 shows a vapor belt distributor, which is intended to uniformly distribute the vapor around the bundle and therefore reduce the excessively large pressure drops and vibration and erosion problems encountered at the vapor inlet end. The shell is extended underneath the vapor nozzle thereby acting as an impingement baffle. Usually, the extended shell within the vapor belt distributor has slots cut around the periphery in order to introduce the vapor into the tube field from all angles. In this case, the open end of the shell shown in the diagram is not needed. The vapor belt distributor is a relatively high-cost construction option but is particularly useful where pressure drop may be a critical consideration.

All vapors introduced into a condenser will contain some amount of non-condensable gas, at least during certain portions of the operational period, whether this composition is shown in the process specifications or not. This fact gives rise to the basic rules for venting condensers: 1. All condensers must be vented. 2. Condensers must be designed to move the non-condensables to a particular point in the condenser by directing the vapor flow path positively through the use of baffles and other mechanical arrangements. 3. The vent must be located where the non-condensables are finally concentrated. 4. A vent condenser may be necessary, sometimes even using a refrigerated coolant, in order to recover as much of the remaining condensable vapor from the non-condensable gas as possible.

It is fair to say that probably half of all operational condenser problems arise from a failure to recognize the basic principles of venting non-condensable gases.

In condensation applications it is frequently necessary to subcool the condensate produced in the condenser. The required amount of subcooling may vary from a few degrees to prevent cavitation in a pump to many degrees required for cooling the condensate to a safe temperature for long-term atmospheric storage. The surest way to carry out the subcooling, especially if large amounts of subcooling are required, is to provide a separate subcooler as shown in Fig. 3.22. In this case, the subcooler is designed as a single-phase heat exchanger with far more precise design methods than are available for integral subcooling calculations. Additionally, the coolant flow rate may be separately controlled to the subcooler giving better control of effluent liquid temperatures. The obvious disadvantage is the generally higher first cost of the separate condenser and subcooler, compared to the cost of the condenser with integral subcooling.

Integral subcooling can be accomplished in a horizontal shell-side condenser by allowing a stratified pool to accumulate in the shell and be sensibly cooled by the inlet coolant, as shown in Fig. 3.23. Some sort of level control (preferably adjustable) is required, and the design calculations are both fairly complex and not very accurate.

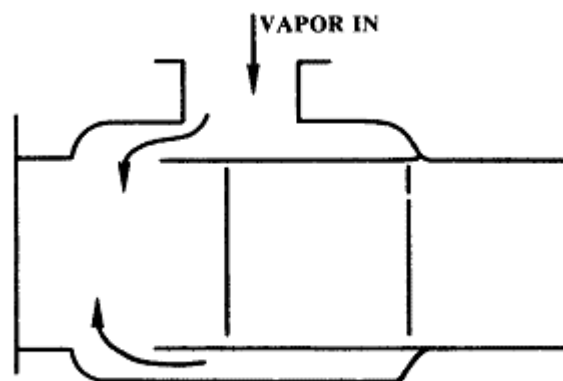


Fig. 3.21 Vapor Belt Distributor.

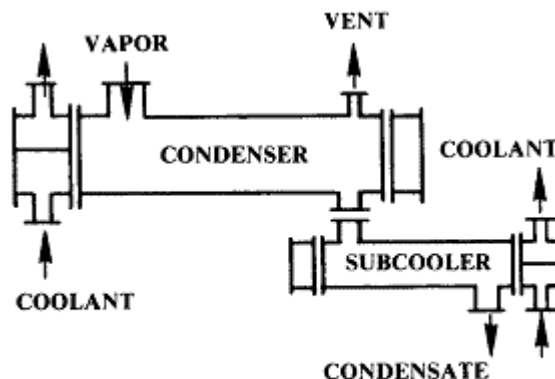


Fig. 3.22 Condenser with Separate Subcooler.



# WOLVERINE TUBE HEAT TRANSFER DATA BOOK

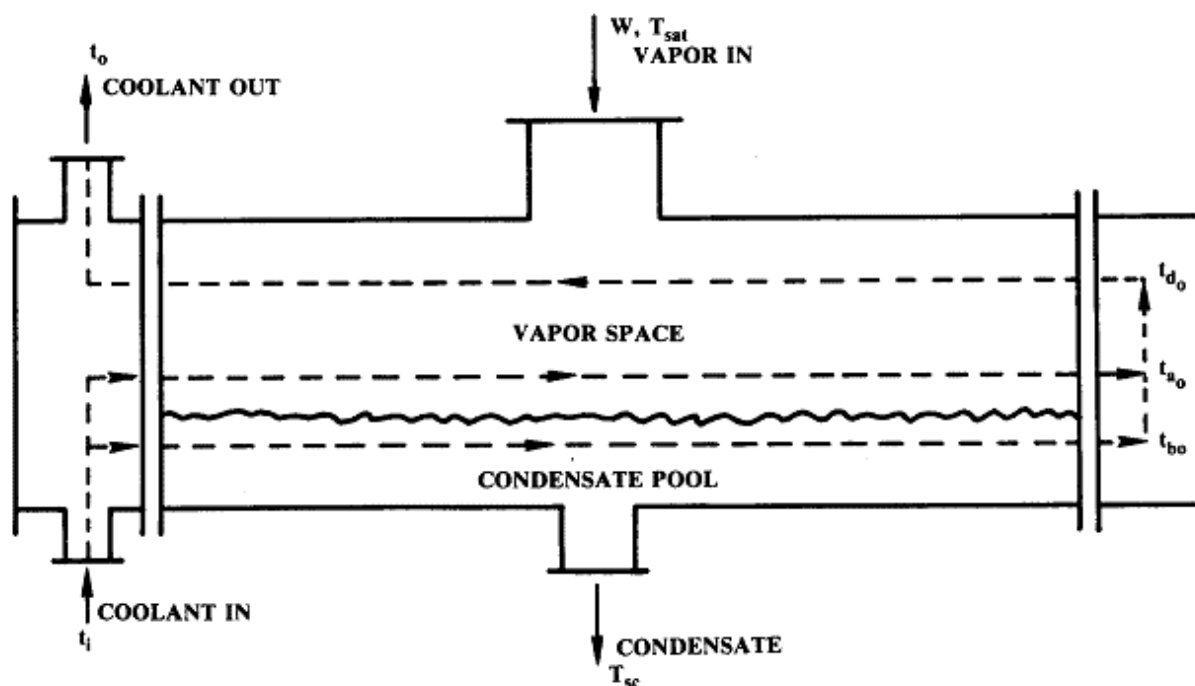


Fig. 3.23 Horizontal Condenser, Shell-Side Condensation, Two-Pass Coolant in Tubes, Arranged for Integral Shell-Side Subcooling.

### 3.3.2. The Basic Design Equations

The basic heat exchanger equations applicable to shell and tube exchangers were developed in Chapter 1, and the reader is referred to that material for the development. Here, we will cite only those that are immediately useful for design in shell and tube heat exchangers with condensing heat transfer on the shell side. Specifically, for the moment, we will limit ourselves to the case when the overall heat transfer coefficient is constant and the other assumptions of the mean temperature difference concept apply. (The important cases of condensation of multi-component vapor or a vapor with a non-condensable gas do not satisfy this requirement and are discussed later.) The basic design equation becomes:

$$Q_T = U^* A^* (\text{LMTD}) \quad (3.54)$$

where  $Q_T$  is the total heat load to be transferred,  $U^*$  is the overall heat transfer coefficient referred to the area  $A^*$ .  $A^*$  is any convenient heat transfer area, and LMTD is the logarithmic mean temperature difference.

$U^*$  is most commonly referred to  $A_o$ , the total outside tube heat transfer area, including fins, in which case it is written as  $U_o$  and is related to the individual film coefficients, wall resistance, etc. by

$$U_o = \frac{1}{\frac{1}{h_o} + R_{fo} + R_{fm} + \frac{\Delta z_w}{k_w} \left( \frac{A_o}{A_m} \right) + R_{fi} \left( \frac{A_o}{A_i} \right) + \frac{1}{h_i} \left( \frac{A_o}{A_i} \right)} \quad (3.55)$$

where  $h_o$  and  $h_i$  are the outside and inside film heat transfer coefficients, respectively,  $R_{fo}$  and  $R_{fi}$  are the outside and inside fouling resistances,  $\Delta z_w$  and  $k_w$  are the wall thickness (in the finned section) and wall



# ***WOLVERINE TUBE HEAT TRANSFER DATA BOOK***

thermal conductivity, and  $R_{fin}$  is the resistance to heat transfer due to the presence of the fin. Since all of the low and medium Trufin tubes manufactured by Wolverine are integral (i.e., tube and fins are all one piece of metal), there is no need to include a contact resistance term.

Suitable correlations for  $h_o$  will be developed in this section. Correlations for  $h_i$  have been developed in Chapter 2. Equations and charts for fin resistance and Wall resistance calculations are found in Chapter 1.

### **3.3.3. Mean Temperature Difference**

The Mean Temperature Difference formulation is detailed in Chapter I but must be used very carefully in condensation applications. For the special but important case of condensation of a pure or nearly pure vapor with negligible pressure drop on the condensing side (i.e., isothermal condensation), the Logarithmic Mean Temperature Difference is not only valid but considerably simplified. If the condensing temperature is  $T_{sat}$  and the inlet and outlet coolant temperature are  $t_1$  and  $t_2$ , then the LMTD (and the MTD) is given by:

$$LMTD = \frac{t_2 - t_1}{\ln \left( \frac{T_{sat} - t_1}{T_{sat} - t_2} \right)} \quad (3.56)$$

(Strictly speaking, since most condensing heat transfer correlations are functions of the local heat flux or the local temperature difference, the LMTD is not exactly valid. However, for practical cases, the effect is small and the use of the LMTD is generally conservative by engineering practice).

If multi-component mixtures or vapors with non-condensable gases are being condensed, or if there are appreciable desuperheating or subcooling effects, the MTD/LMTD formulation is not valid. Special techniques need to be used for these cases; these are described later.

### **3.3.4. Condensation of a Superheated Vapor**

It is often necessary to condense a vapor whose inlet temperature is above the saturation temperature at the pressure existing in the condenser. Such a case can arise with exhaust vapor from a non-condensing turbine or a vapor throttled through a valve. There is some confusion in the literature about the proper way to design for condensing a superheated vapor, but the following argument [shortened from Ref. (17)] is generally accepted as correct.

If the vapor entering a condenser is superheated, the sensible heat content of the vapor must be removed and transferred through the cooling surface before that vapor can be condensed. If the cold surface is above the saturation temperature of the vapor, the heat is removed by a convective sensible heat transfer mechanism, the coefficient for which can be calculated from a correlation applicable to the geometry involved and employing vapor physical properties. However, if the cold surface is below the saturation temperature of the vapor at the existing pressure, vapor will condense directly upon the surface with essential thermodynamic equilibrium existing at the condensate-vapor interface and with the temperature gradient from the superheated state to saturation occurring in the vapor immediately adjacent to the interface.

The information available [Refs. (18,19)] indicates that the heat transfer coefficient for condensation directly from the superheated vapor is within a few percent of that for condensation from the saturated





# WOLVERINE TUBE HEAT TRANSFER DATA BOOK

vapor, using the saturation temperature of the vapor to calculate the temperature difference for heat transfer.

To determine whether or not condensation will occur on a cold surface exposed to superheated vapor, first assume that heat is transferred from the superheated vapor by sensible heat transfer. If  $T_v$  is the local vapor temperature,  $T_{sat}$  the condensing or saturation temperature, and  $t$  the local coolant temperature, then the surface temperature on the vapor side,  $T'_s$ , is given by

$$T'_s = T_v - \frac{U_s(T_v - t)}{h_s} \quad (3.57)$$

where  $h_s$  is the sensible heat transfer coefficient for the vapor stream and  $U_s$  is the overall coefficient computed using  $h_s$ . If  $T'_s > T_{sat}$ , no condensation will occur,  $T'_s$  is equal to the true surface temperature  $T_s$ , and the heat transfer rate is given by  $(Q/A) = U_s(T_v - t)$ . If  $T'_s < T_{sat}$  condensation will occur and the heat transfer rate is given by  $(Q/A) = U_c(T_{sat} - t)$ , where  $U_c$  is the overall coefficient computed assuming condensation does occur, and the true surface temperature is given by

$$T_s = T_{sat} - \frac{U_c(T_{sat} - t)}{h_c} \quad (3.58)$$

In this case,  $U_c = U_o$  as given by Eq. (3.55), with  $h_o$  in that equation being the same as  $h$  in the above discussion. Correlations for the  $h_c$  are given later.

There is a further consequence. Define  $U'$  as the combined heat transfer coefficient for the wall resistance, the coolant, and any dirt film.  $U'$  is essentially independent of the heat flux and whether or not condensation is occurring on the outer surface. Then the heat flux for the sensible heat transfer desuperheating case is  $(Q/A)_s = U'(T'_s - t)$  and that for the condensing case is  $(Q/A)_c = U'(T_s - t)$ . Since  $T'_s > T_{sat} \geq T_s$ ,  $(Q/A)_s > (Q/A)_c$ . Therefore, condensation will occur directly from the superheated vapor, unless a higher heat flux is obtained by the sensible heat transfer mode. A corollary to this is that it is both simpler and more conservative (in the sense of calculating a larger condenser area) to assume that condensation will occur directly from the superheated vapor, using the saturation temperature and a condensing heat transfer coefficient in the rate equation, and of course including the sensible heat in the heat load.

### 3.3.5. Condensation with Integral Subcooling On the Shellside

Condensate subcooling is frequently required to provide the NPSH for a pump or to cool a product for a surge tank or for storage. Usually this subcooling is best done in a separate sensibly cooling heat exchanger, specifically designed for this purpose. It should also be remembered that filmwise condensation results in a liquid film that is subcooled on the order of 1/3 to 1/2 of  $(T_{sat} - T_s)$ . If reheating can be avoided and the pump judiciously located, this subcooling may be sufficient for the purpose.

Occasionally, however, it may be desirable, especially if a moderate degree of subcooling is required, to provide a region in a horizontal condenser shell where the condensate may exchange heat with the cold coolant entering. In this case, a rational approach to calculating the subcooling area required is necessary. Referring to Fig. 3.23, the surface of the liquid pool is shown as essentially horizontal, whereas in reality pressure differences may cause considerable hydrostatic gradient. In this case, the value of  $F$  calculated later must be understood to be the *effective* fraction of tubes flooded.



# WOLVERINE TUBE HEAT TRANSFER DATA BOOK

In the absence of better knowledge, the pool can be conservatively assumed to be isothermal at  $T_{sc}$  the desired subcooling temperature. The condenser therefore may be envisioned as composed of two regions, each isothermal on the shell side: 1) the condensing region at  $T_{sat}$  and 2) the subcooling region at  $T_{sc}$ . The heat load and temperature profile of the coolant as a function of length are then given by

$$Q(x) = wc_p (t - t_i) \quad (3.59)$$

$$= U_{sc} ax \frac{t - t_i}{\ln \left( \frac{T_{sc} - t_i}{T_{sc} - t} \right)} \quad (3.60)$$

in the subcooling region, where  $t$  is the temperature of the coolant at any distance  $x$  down the tube. Solving for  $t$  gives

$$t = T_{sc} - (T_{sc} - t_i) e^{-\frac{U_{sc} ax}{wc_p}} \quad (3.61)$$

At the end of the tube,  $x = L$ , and  $t$  is the outlet temperature for that pass,  $t_{bo}$  in the case diagrammed in Fig. 3.23. An analogous equation holds for the condensing region, resulting in a tube outlet temperature of  $t_{ao}$  from the tubes in the first pass that are in condensing service. At the turnaround, the two streams from the first pass are presumed to mix completely to give  $t_{do}$  by heat balance, which becomes the inlet temperature for the next pass. In the use of Eq. (3.61) it is immaterial whether  $aL$  is taken to be the area per tube and  $w$  the coolant flow rate per tube or whether  $aL$  is the total area of all tubes in a pass and  $w$  the total coolant flow rate. In the following computational scheme, the latter viewpoint is adopted together with the fact that in a two-pass configuration (with equal tubes/pass)  $aL = A_T/2$ , where  $A_T$  is the total tube surface area in the bundle.

The algorithm for this case proceeds by estimating the total area required (step 3) and determining whether the final outlet temperature of the coolant is equal to that required by the heat balance. The total area is then adjusted until the temperatures do match. Since step 3 provides only a very rough estimate, it is possible that the  $A_T$  thus predicted will throw the first sequence of calculations into the wrong branch, especially if  $F$  (step 5) is near 1. This is readily detected by inspection during the calculations and a more realistic value of  $A_T$  can be estimated at steps 9 or 15. The computational sequence is:

1. Calculate the heat loads.

$$Q_c = W\lambda \quad (3.62)$$

$$Q_{sc} = WC_p(T_{sat} - T_{sc}) \quad (3.63)$$

2. Calculate the coolant flow rate.

$$w = \frac{Q_c + Q_{sc}}{c_p(t_o - t_i)} \quad (3.64)$$

3. Estimate the total area.



# WOLVERINE TUBE HEAT TRANSFER DATA BOOK

$$A_T \approx \frac{Q_c}{U_c \left[ \frac{t_o - t_i}{\ln \left( \frac{T_{sat} - t_i}{T_{sat} - t_o} \right)} \right]} + \frac{2 Q_{sc}}{U_{sc} (T_{sc} - t_i)} \quad (3.65)$$

4. Calculate the outlet temperature from the flooded tubes in the first pass.

$$t_{bo} = T_{sc} - (T_{sc} - t_i) e^{-\frac{U_{sc} A_T}{2wc_p}} \quad (3.66)$$

5. Calculate the fraction of tubes in the first pass to be flooded, F.

$$F = \frac{Q_{sc}}{wc_p (t_{bo} - t_i)} \quad (3.67)$$

If  $F > 1$ , the entire first pass is to be flooded; go to step 10 directly.

6. Calculate the outlet temperature from the unflooded tubes in the first pass.

$$t_{ao} = T_{sat} - (T_{sat} - t_i) e^{-\frac{U_c A_T}{2wc_p}} \quad (3.68)$$

7. Calculate the mixed mean outlet temperature from all the first pass tubes.

$$t_{do} = (1 - F)t_{ao} + Ft_{bo} \quad (3.69)$$

8. Calculate the outlet temperature from the second pass (and hence from the condenser.)

$$t_o^* = T_{sat} - (T_{sat} - t_{do}) e^{-\frac{U_c A_T}{2wc_p}} \quad (3.70)$$

9. Does  $t_o^* = t_o$  specified?

Yes: Total condenser – subcooler area required is  $A_T$  and F of the first pass tubes are to be flooded.

No: Assume new  $A_T$  and go to step 4.

10. Calculate the exit temperature from the first-pass tubes, all of which are flooded.

$$t_{eo} = T_{sc} - (T_{sc} - t_i) e^{-\frac{U_{sc} A_T}{2wc_p}} \quad (3.71)$$

11. Calculate the exit temperature from the second-pass tubes that are flooded.

$$t_{fo} = T_{sc} - (T_{sc} - t_{eo}) e^{-\frac{U_{sc} A_T}{2wc_p}} \quad (3.72)$$



# WOLVERINE TUBE HEAT TRANSFER DATA BOOK

12. Calculate the exit temperature from the second-pass tubes in condensing service.

$$t_{go} = T_{sat} - (T_{sat} - t_{eo})_e \frac{U_c A_T}{2wc_p} \quad (3.73)$$

13. Calculate the fraction of second pass tubes that are in condensing service.

$$F' = \frac{Q_c}{wc_p(t_{go} - t_{eo})} \quad (3.74)$$

14. Calculate the mixed-mean temperature from the second-pass tubes.

$$t^* = F't_{go} + (1 - F')t_{fo} \quad (3.75)$$

15. Does  $t_o^* = t_o$  specified?

Yes: Total condenser-subcooler area required is  $A_T$  and all but  $F'$  of the second pass tubes are to be flooded, i.e.  $(1-F'/2)$  of all the tubes in both passes are to be flooded.

No: Assume new  $A_T$  and go to step 10.

If U tubes are used in the condenser-subcooler, no mixing of the tube side fluid occurs at the end of the first pass. Assume that the tubes are all the same length and have the same effective heat transfer area; this is not strictly true, but is a convenient assumption and one well within the normal bounds of error for both this case and for other U-tube applications.

The first six steps in the computational scheme are identical with the previous analysis. Then the scheme proceeds as follows:

7. Calculate the outlet temperature from the second pass tubes that were flooded in the first pass.

$$t_{jo} = T_{sat} - (T_{sat} - t_{bo})_e \frac{U_c A_T}{2wc_p} \quad (3.76)$$

8. Calculate the outlet temperature from the second pass tubes that were in condensing service in the first pass.

$$t_{ko} = T_{sat} - (T_{sat} - t_{ao})_e \frac{U_c A_T}{2wc_p} \quad (3.77)$$

9. Calculate the mixed mean outlet temperature from all the second pass- tubes (and hence from the condenser).

$$t_o^* = F t_{jo} + (1 - F) t_{ko} \quad (3.78)$$

- 9A. Does  $t_o^* = t_o$  specified?

Yes: Total condenser-subcooler area is  $A_T$  and  $F$  of the first pass tubes are to be flooded.



# WOLVERINE TUBE HEAT TRANSFER DATA BOOK

No: Assume new  $A_T$  and go to step 4.

Steps 10- 15 for this case (corresponding to all of the first pass tubes being flooded) are identical to those for the previous case.

## 3.3.6. Filmwise Condensation on Plain and Trufin Tubes

The development of the equations for condensing outside of tubes is based on the same Nusselt model and assumptions that were discussed in detail in the analysis for in-tube condensing. These led to the development of Eq. (3.45) for condensing inside a horizontal tube. By replacing  $d_i$  in the equation with  $d_o$  the following equation is obtained:

$$h_c = 0.725 \left[ \frac{k_\ell^3 \rho_\ell (\rho_\ell - \rho_v) \lambda g}{\mu_\ell d_o (T_{sat} - T_w)} \right]^{1/4} \quad (3.79)$$

where  $h_c$  is the average condensing heat transfer coefficient on the outside of the tube. Further,  $k_\ell$  and  $\mu_\ell$  are respectively the thermal conductivity and viscosity of the condensate,  $\rho_\ell$  and  $\rho_v$ , the densities of condensate and vapor respectively,  $\lambda$  the latent heat of condensation,  $g$  the gravitational acceleration,  $d_o$  the outside diameter of the tube,  $T_{sat}$  the saturation temperature of the vapor and  $T_w$  the wall temperature.

The equation may also be written as:

$$h_c = 0.951 \left[ \frac{k_\ell^3 \rho_\ell (\rho_\ell - \rho_v) g L}{\mu_\ell W} \right]^{1/3} \quad (3.80)$$

where  $L$  is the length of the tube and  $W$  is the mass of vapor condensed on the tube per unit time. Other forms of the equation are possible.

These equations are found to predict actual heat transfer coefficients on horizontal single plain round tubes quite closely, on the average about 15 percent lower than the experimental values. The difference is usually attributed to rippling of the film and early turbulence and drainage instabilities on the bottom side of the tube. The equation can also be used with some modification to predict condensing coefficients on Trufin tubes.

Condensation on horizontal low-finned tubes was studied experimentally by Beatty and Katz (20) who found that the data could be correlated by a modified form of Eq. (3.79):

$$h_c = 0.689 \left[ \frac{k_\ell^3 \rho_\ell (\rho_\ell - \rho_v) \lambda g}{\mu_\ell (T_{sat} - T_w)} \right]^{1/4} \left( \frac{1}{d_{eq}} \right)^{1/4} \quad (3.81)$$

where



# WOLVERINE TUBE HEAT TRANSFER DATA BOOK

$$\left(\frac{1}{d_{eq}}\right)^{1/4} = 1.3\Phi \frac{A_{fin}}{A_{eq}} \left(\frac{1}{\bar{L}}\right)^{1/4} + \frac{A_{root}}{A_{eq}} \left(\frac{1}{d_r}\right)^{1/4} \quad (3.82)$$

where  $\Phi$  is the fin efficiency,  $A_{fin}$  is the total fin area,  $A_{eq}$  is the effective outside area of a finned tube,  $A_{root}$  is the plain tube outside heat transfer area (based on root diameter), and  $d_r$  is the root diameter.  $L$  is defined by:

$$\bar{L} = \frac{a_{fin}}{d_o} \quad (3.83)$$

where  $a_{fin}$  is the area of one side of one fin,

$$a_{fin} = \frac{\pi}{4} (d_o^2 - d_r^2) \quad (3.84)$$

The fin efficiency can be calculated from:

$$\Phi = \frac{1}{1 + \frac{m^2}{3} \sqrt{\frac{d_o}{d_r}}} \quad (3.85)$$

where

$$m = H \sqrt{\frac{2}{\left(\frac{1}{h_o} + R_{fo}\right) k_w Y}} \quad (3.86)$$

also,

$$A_{fin} = \frac{\pi}{2} (d_o^2 - d_r^2) N_f L \quad (3.87)$$

where  $N_f$  is the number of fins per unit length and  $L$  is the finned length of the tube,

$$A_{eq} = \Phi A_{fin} + \pi d_r L \left( \frac{s}{s+Y} \right) \quad (3.88)$$

and

$$A_{root} = \pi d_r L \left( \frac{s}{s+Y} \right) \quad (3.89)$$

The above set of equations is quite accurate for calculating the heat transfer coefficient on Trufin. However, it is also rather awkward to use, and it has been found as a practical matter that a much simpler and nearly as good a result can be obtained by the use of Eq. (3.79) using  $d_r$  as the diameter and applying the value of  $h_c$  thus found to the entire outside finned tube surface  $A_o$ .





# WOLVERINE TUBE HEAT TRANSFER DATA BOOK

$$A_o = \pi L \left[ d_r \left( \frac{s}{s+Y} \right) + \frac{1}{2} (d_o^2 - d_r^2) N_f \right] \quad (3.90)$$

Alternatively, Eq. (3.80) can be used to calculate  $h_o$ . Use of either equation is in principle a trial and error calculation, and the actual procedure is later illustrated by an example problem.

In the application of all of these equations, it must be remembered that Trufin tubes should not be used for condensing steam. Water has a high surface tension and the condensate film will bridge the fins. The thick layer of liquid thus held in place on the tube acts as an insulator; the resulting heat transfer rate per unit length of tube is substantially less than for a plain tube. It is not clear at what value of the surface tension this effect becomes significant. Condensates with surface tensions as high as 25-30 dyne/cm have been condensed on finned tubes with no reported difficulty; this includes the usual design range for hydrocarbons, alcohols, refrigerants, etc., with surface tensions from 10 to 25 dyne/cm. However, there is a severe penalty for the condensation of water at atmospheric pressure, at which the surface tension is about 60 dyne/cm. No data or reported experience appears to exist in between.

### 3.3.7. Filmwise Condensation on Tube Banks

#### 1. Effect of number of rows of tubes.

In any practical condenser design the condensate formed on tubes near the top of the bundle will fall on tubes lower in the bank and presumably modifying the heat transfer coefficient. Nusselt (7) assumed undisturbed laminar flow on each successive tube and found theoretically that the average condensing heat transfer coefficient for a bank of horizontal plain tubes is given by:

$$h_{c,N} = h_{c,1} N^{-1/4} \quad (3.91)$$

where  $h_{c,1}$  is the heat transfer coefficient for one row calculated by the previous equations and  $N$  is the number of tubes in one vertical row. For a reasonable size process condenser  $N$  may be 20 or 30, and this equation predicts a very severe penalty compared to a single tube. Kern (21) recommended an exponent of  $(-1/6)$ , again for plain tubes. However, Short and Brown (22) experimentally found no net penalty against the single tube coefficient in a single row 20 tubes high.

The latter result is generally borne out in process experience, and current design practice is to assume that the average coefficient for the entire tube bank is the same as for a single tube. The explanation generally advanced is that rippling, splashing, and turbulence induced by liquid falling from one tube to the next overcomes the possible disadvantages of an increasing liquid loading on each tube.

#### 2. Effect of vapor shear.

It is well known that vapor flowing at a high velocity across the tubes can increase the heat transfer coefficient significantly above the theoretical gravity-driven flow model of Nusselt. However, very few data actually exist to estimate the significance of the effect and most of these data are proprietary. One

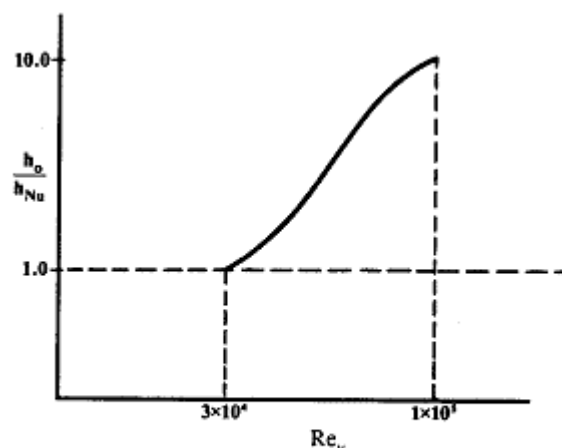


Fig. 3.24 Effect of Vapor Shear on Condensing Heat Transfer in a Tube Bank.



# WOLVERINE TUBE HEAT TRANSFER DATA BOOK

widely-cited graph, Fig. 3.24, indicates that the heat transfer coefficient becomes greater than the Nusselt value at vapor Reynolds numbers above about 30,000, increasing to about 10 times as much at  $Re_v = 100,000$ . However, all data are for plain tube banks and often at vapor velocities so high that excessive pressure drops would be required to achieve significant improvement. Until more data are available, it appears prudent to calculate condensing coefficients as if the flows were purely gravity-driven.

### 3.3.8. Pressure Drop during Shell Side Condensation

Very few data have been published for pressure drop during condensation on the shell-side of the shell and tube heat exchanger. Diehl and Unruh (23, 24) presented a correlation for two-phase adiabatic (i.e., no phase change) pressure drop across several tube banks in both vertical downwards and horizontal cross flow for an ideal tube bank.

Making certain assumptions, Brooks (25) worked from the Diehl-Unruh correlations to obtain a correction factor converting the calculated shell-side pressure drop for the all-vapor flow to the pressure drop for a condenser with a saturated vapor inlet and an exit vapor quality  $x_o$ . This figure is given here as Fig. 3.25.

In order to use Fig. 3.25, one must first calculate the shell side pressure drop for the all-vapor flow, using the method given in Chapter 2. Since that method is quite lengthy to present, it will not be repeated here. Then the pressure drop for the all-vapor flow is multiplied by the correction factor  $\Phi_{gt}^2$ , from Fig. 3.25 for the appropriate exit quality from the condenser.

Several assumptions have been made in obtaining Fig. 3.25, among the more important being:

1. The shell-side vapor flow is always turbulent.
2. All tube bank layouts have the same correction factor. (Diehl and Unruh found that the  $45^\circ$  banks give somewhat higher pressure drops than the  $60^\circ$  and  $90^\circ$  banks in the liquid-rich end, where the pressure gradient is less anyway. The present curve is based on the mean of the results.)
3. The effect of two-phase flow on pressure drop in the windows is similar to that in crossflow.
4. The rate of condensation is constant through the length of the bundle. A partial condenser that has a higher condensation rate near the entrance should give a lower pressure drop than estimated by Fig. 3.25 and vice versa.

It should be recognized that the calculation of shell-side pressure drop is at best a rough estimation and that too little testing has been done against actual condensers to allow for a more precise method.

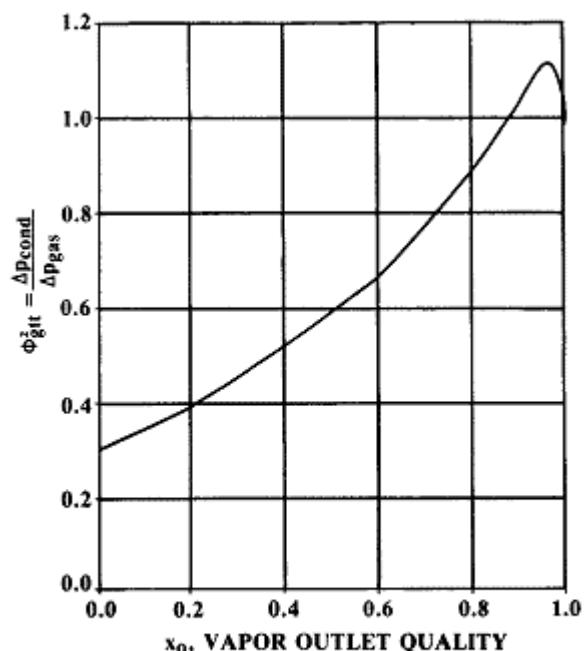


Fig. 3.25 Correction Factor for Shell Side Condenser Pressure Drop.